Magnetic Field-Assisted Electroless Anodization: TiO_2 Nanotube Growth on Discontinuous, Patterned Ti Films

Arash Mohammadpour[1] and Karthik Shankar[1,2]

[1] Department of Electrical and Computer Engineering, University of Alberta, Edmonton, AB, T6G 2V4, Canada
[2] National Institute for Nanotechnology, National Research Council, 11421 Saskatchewan Drive, Edmonton, AB, T6G 2M9, Canada

Abstract

We present a magnetic field-assisted oxidation and etching process that transforms Ti thin films on arbitrary substrates into self-organized TiO_2 nanotube arrays without the direct application of an anodization voltage between the cathode and the Ti film/substrate. In effect, the Ti film/substrate electrode is at a floating potential determined by the ionic Hall voltage. The development of such a magnetic field-assisted electroless anodization process, frees the anodization technique of forming nanostructured semiconductors and metal oxides from the constraints of substrate conductivity and film continuity imposed by the traditional anodization process, and allows the creation of uniform anodic nanostructures on pre-existing high-aspect ratio patterns as well as on substrates containing both conductive and non-conductive areas. Using magnetic field assisted electroless anodization, we demonstrate the formation of microscale patterns of high quality TiO_2 nanotubes from discontinuous Ti films deposited on thermal oxide-coated Si substrates and patterned by a lift-off process.

Keywords electrochemical anodization, Lorentz force, ionic Hall effect, nanopores, valve metal oxide, porous Si, III-V semiconductors, photocatalysts, solar cells, sensors, supercapacitors.

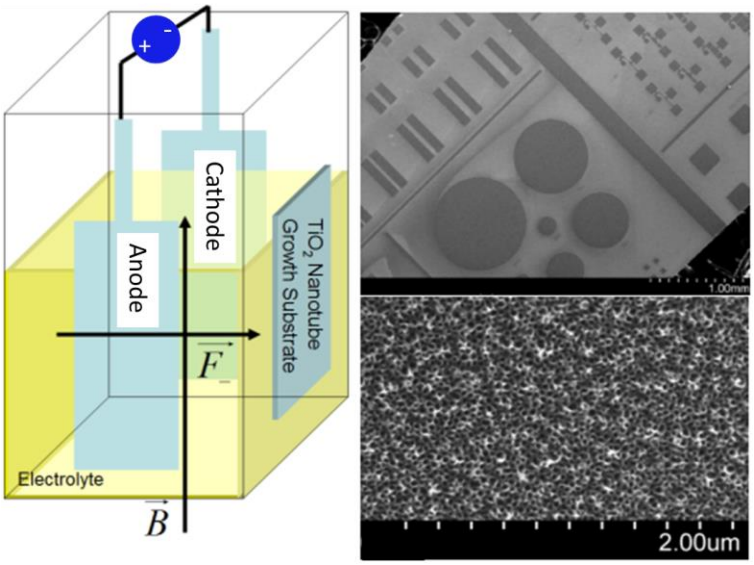

(*TOC Graphic*)

Introduction

The potential of nanomaterials to offer unique properties and improved performance in a variety of sensing, energy harvesting and biomedical applications is responsible for the intense research activities in nanoscience and nanotechnology. From the very beginning, it has always been recognized that interfacing nanostructures with the macroscopic world to utilize their full potential would require the use of microstructures as intermediaries. However in many cases, techniques to perform such interfacing have lagged behind advances in the synthesis and property-engineering of nanomaterials. For instance, there has been impressive progress in controlling the geometrical and morphological properties of anodically formed TiO_2 nanotube arrays (length, wall thickness, pore diameter and pattern order)[1-3] over a very wide range, as well as generating more complex structures (multipodal[4], hierarchical[5] and periodically modulated TiO_2 nanotube arrays[6-8]) by optimizing anodization parameters such as applied voltage, electrolyte composition, temperature, pH and anodization time. Although such self-organized, vertically oriented TiO_2 nanotube (TNT) arrays have been found to be promising for deployment in liquid junction dye-sensitized and solid-state ordered heterojunction solar cells,[9-16] water photoelectrolysers and photocatalysts,[17-19] supercapacitors,[20-23] gas sensors,[24-26] stem cell differentiators,[27-29] glucose sensors,[30, 31] biomarker assays[32, 33] and drug delivery,[34-36] very little progress has been made in integrating TNTs with microsystems.

The main obstacle for integration and interfacing with microscale structures has been the requirement of a continuous, conducting, vacuum deposited thin film of Ti as a necessary pre-requisite for subsequent anodic transformation into TiO_2 nanotubes (Fig. 1). In applications such as micromachined resonators, TNT arrays are often sought to be formed on high-aspect ratio features as depicted in Fig. 1a. When narrow gaps critical to device operation are present

between high aspect ratio features, as is often the case with lateral resonators and comb-drives, the process of vacuum deposition to form the precursor Ti films closes the narrow gaps (Figs. 1b and 1c), which are very difficult to subsequently re-open following the formation of TiO_2 nanotubes. When wide gaps are present between adjacent high-aspect ratio features, thermal evaporation of the titanium film results in discontinuous films due to poor step coverage, thus terminating the anodization process (Fig. 1 b). Sputtering Ti films results in better step coverage compared to evaporation, but the lower film thickness along the step-walls and non-uniform electric field distribution result in non-uniform nanotube formation and/or film discontinuities due to certain areas of the Ti film fully transforming into insulating TiO_2 before others (Fig. 1c). This illustrates the near-incompatibility of the currently used TNT growth process with high-aspect ratio micromachining. These problems, while reduced in severity, are nevertheless present even for low-aspect ratio micromachining. Another source of problems during integration and interfacing of the microscale with the nanoscale is the non-uniform growth of TiO_2 nanotubes on a substrate containing both conductive and non-conductive areas. Fig. 1d illustrates a configuration consisting of TNT arrays on metal electrodes separated by a dielectric, one that is often required to make electrical contact to the nanotube arrays. A key problem in transforming a Ti film deposited on such a hybrid metal-dielectric surface is that the areas above the metal electrodes experience faster rates of anodization due to the higher conductivity resulting in non-uniform TNT arrays (Figs. 1e and 1f).

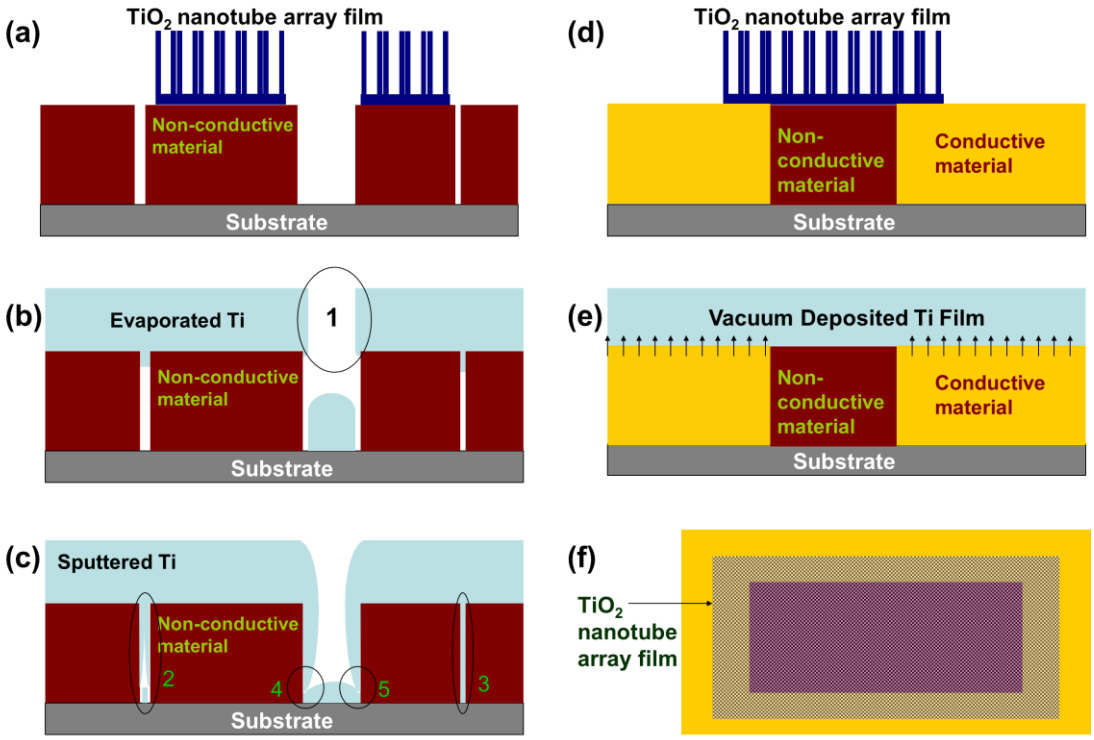

Fig. 1 Schematic illustrations of patterned and micromachined cross-sections (a) Desired configuration of metal oxide nanotube arrays in defined areas of a substrate over patterned high-aspect ratio features (b, c) Profile generated by vacuum deposition of Ti on to a patterned surface containing high-aspect ratio features separated by wide and narrow gaps (d, e, f) Desired configuration, field and conduction non-uniformities, and expected top-view for nanotube arrays over a composite surface. See text for further explanation.

In order to achieve more structural complexity in TiO_2 nanotube arrays for present and emerging application, introducing new parameter(s) to achieve this goal is much needed, especially because on the synthetic side, exploration of the parameter space associated with the existing variables of the anodization process, such as anodization potential, anodization duration and sequencing, type of electrolyte, bath temperature, etc. is approaching exhaustion. Herein we report on introducing magnetic fields for the first time into the process of anodization to form TiO_2 nanotube arrays. Magnetic fields have been used in the electrochemical synthesis of nanomaterials such as porous silicon and porous III-V semiconductors, but never without direct

connection to an electrode in the manner we have described. In all magnetic-field-assisted anodization processes reported thus far, an electrode was connected to the sample during anodization and the external magnetic field was applied to improve a structural property. Such a configuration has been utilized mostly in generating porous Si (PS) in which an applied magnetic field led to morphological improvement of porous structure,[37] significant increment in photoluminescence intensity of PS[38] and higher porosity.[38] Magnetic fields have been also reported to enhance the controllability of periodic silicon nanostructures[39] and were also exploited in the formation of hole arrays on GaAs surfaces.[40] The innovation in our method relies on the fact that the Ti coated sample is free-standing into the electrolyte and ions are directed towards it using an external magnetic field to generate TiO_2 nanotube arrays. In other words, anodization occurs purely due to the Lorentz-force guided oxidation and etching of Ti/TiO_2 by ions, which releases the anodization process from the constraint of Ti film continuity and the requirement of either the film or substrate to be conductive. The conventional anodization method possesses several drawbacks. Continuity of the deposited Ti film is required when growing TiO_2 nanotubes on various substrates. Hence, nanotube growth through anodization of discontinuous/patterned Ti on a non-conducting substrate is impossible. Herein we show that magnetic-field-assisted anodization can be used to grow nanotubes from a patterned, discontinuous Ti film on a substrate that is at a floating potential in the electrolyte.

Experimental

Anodization was performed at room temperature in an ethylene glycol (EG)-based electrolyte containing 0.3 wt.% NH_4F and 2 vol.% deionized water at 50 V. The electrochemical cell

consisted of a 1-cm spectroscopic cuvette adapted to this experiment. The sample that was sought to be used as a virtual electrode to grow TiO_2 nanotube arrays, was fully immersed into the electrolyte and attached to one of the walls of the cuvette using Kapton tape. The samples used were Ti foils as well as continuous and patterned, discontinuous Ti thin films deposited on different substrates. Patterned substrates containing discontinuous Ti films were created by depositing 400 nm of Ti onto the photolithographically defined features in HPR 504 photoresist by electron beam evaporation and then removing the unwanted metal by lift-off. The electrodes to which a potential difference (using a DC power supply) was applied to produce motion of the ions in the electrolyte were two rectangular Ti foils 5.5 cm x 0.6 cm in size, which were placed against two opposite walls of the cuvette adjacent to the sample wall, with 3.7 cm of their length immersed into the electrolyte. In some cases the surface area of the Ti electrodes was adjusted by covering some areas with parafilm to create windows of defined size exposed to the electrolyte and also to reduce high local electric fields at electrode edges and interfaces. Ti foils were ultrasonically cleaned using Micro-90 solution, deionized water, acetone and isopropanol for 10 min each. The cuvette cell was placed onto a stack of neodymium permanent magnets with magnetic fields of ranging from 0 to 0.84 tesla in total. The magnetic field strength at the sample was measured using a DC Gaussmeter model 1-ST (Alphalab). The orientation of the magnetic fields was perpendicular to the plane of the magnets and therefore, the magnetic field was directed from bottom to the top of the cuvette. The morphologies of the samples subsequent to anodization were imaged using JEOL6301F and Hitachi S4800 field emission scanning electron microscopes (FESEM). Optical micrographs were obtained using an Axio Lab.A1 microscope (Zeiss) at magnifications of 10-50X. The anodization current densities were measured using a Keithley 4200 semiconductor parameter analyzer and PC-Link multimeter.

Results

Fig. 2 shows SEM images of three Ti foils placed at different positions in the cuvette cell during magnetic-field-assisted anodization. Looking into the erect electrolyte-filled cuvette from the cathode side, the three Ti foils were placed as follows: one foil at the left-hand-side (LHS) of the cathode while no electrode was connected to it, a second foil in front of and opposite to the cathode while electrically connected to the positive terminal of the power supply and a third foil at the right-hand-side (RHS) of the cathode with no electrode connection respectively. Nanotube growth on the LHS foil occurs without any electrode connection (Fig. 2a), and is attributed to the negative ion deflection towards the foil using Lorentz force generated by external magnetic field. These negative ions include both film forming, oxidizing species such as OH^- and O^{2-}, and film etching species such as F^-. The magnetic field oriented along the height of the cuvette from the bottom to top, was responsible for steering the negatively charged oxide, hydroxide and fluoride ions to the left while they were transiting from cathode to anode under the influence of the applied electrochemical voltage. The Hall voltage thus set-up by the magnetic field-induced an asymmetric distribution of ionic charge carriers and produced virtual electrodes on either side of the cathode. In general, titania nanotube growth occurs due to the simultaneous occurrence of field-assisted oxidation, migration and dissolution processes. The OH^- and O^{2-} ions deflected toward the LHS electrode can produce oxidation and similarly deflected F^- ions can produce dissolution. Instead of the oxidation and dissolution processes being field-assisted, they are now assisted by the momentum of the impinging ions. However the sign of the Hall voltage is such as to oppose further movement of negative charge toward the virtual electrode. The electric field that results across the LHS Ti foil-electrolyte interface is opposite to that required for the migration of positive ions. This suggests that field-assisted migration of positively charged ions

is almost absent in the process discussed and provides the further insight that field-assisted migration of positively charged metal ions from the Ti bulk toward the electrolyte interface is not essential to the nanotube growth process. Nanotube growth on the Ti foil opposite the cathode constituting the anode of the circuit merely confirms the conventional anodic formation of TiO_2 nanotubes (Fig. 2b). The importance of the Lorentz force was verified by the absence of nanotube formation at the RHS foil (top-view SEM image in Fig. 2c) toward which only positive ions are deflected.

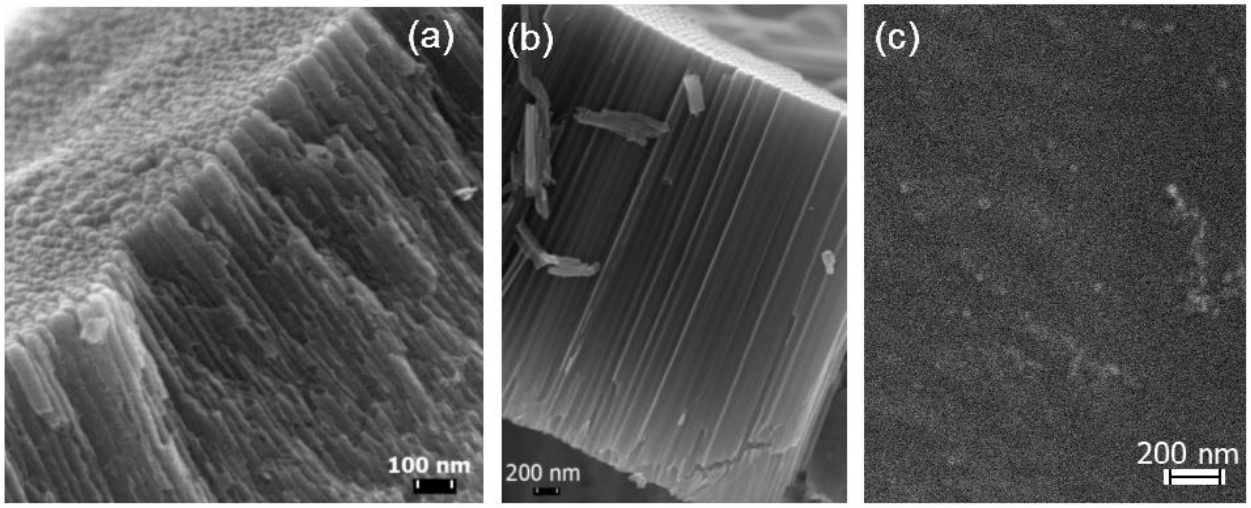

Fig. 2 SEM images of Ti foils anodized in presence of magnetic field and placed into the cuvette a) at left-hand-side of the cathode (no electrode connected) b) in front of cathode (connected to the anode electrode) and c) at right-hand-side of the cathode (no electrode connected).

Lorentz force deflecting the accelerating negatively charged ions was location dependent due to velocity variation of the ions at different spots in the electrolyte. This could reduce the order range of the generated TiO_2 nanotube arrays (Fig. 2a).

Being able to fabricate TiO_2 nanotube arrays onto a substrate without any electrical connection is advantageous since it opens a way forward to grow nanotube arrays through the

anodization of discontinuous Ti films deposited on substrates of any conductivity. To verify this possibility, we subjected a patterned, discontinuous Ti film to the same magnetic-field assisted anodization process. Fig. 3 is a schematic of the experimental configuration used for this experiment.

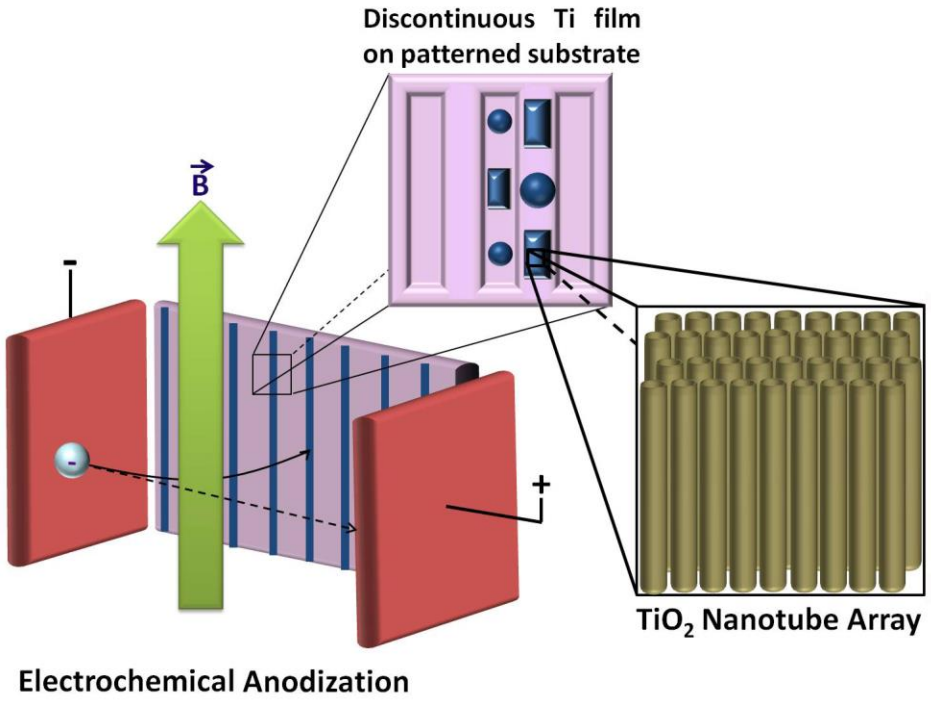

Fig. 3 Cartoon showing patterned, discontinuous Ti film sample without any direct electrical connection placed along the wall in the cuvette electrochemical cell on the left hand side (LHS) of the cathode. The Ti on the LHS sample is transformed into TiO_2 nanotubes upon magnetic field-assisted virtual anodization.

Fig. 4a shows the optical microscope image of a 400 nm-thick discontinuous Ti film deposited onto Si substrate. The patterned sample was placed against the LHS wall of the cuvette electrochemical cell with no electrode connection while both cathode and anode were Ti foils. Figs. 4b and 4c show SEM images of two different patterns comprised of anodized TiO_2 nanotube arrays in which SEM insets represent higher magnification images of gap area,

confirming the magnetic field-assisted formation of TNT arrays from discontinuous Ti films on arbitrary substrates. Lower SEM inset in Fig. 4b show the nanotube arrays after top debris layer was etched away using SF_6 gas through reactive ion etching (RIE). Color images in the insets of Figs. 4b and 4c are optical micrographs obtained after anodization in which the variation in the color due to optical interference is a distinctive indication of the presence of an anodized oxide film. Cross-sectional SEM image of the grown discontinuous TiO_2 nanotube arrays is depicted in Fig. 4d.

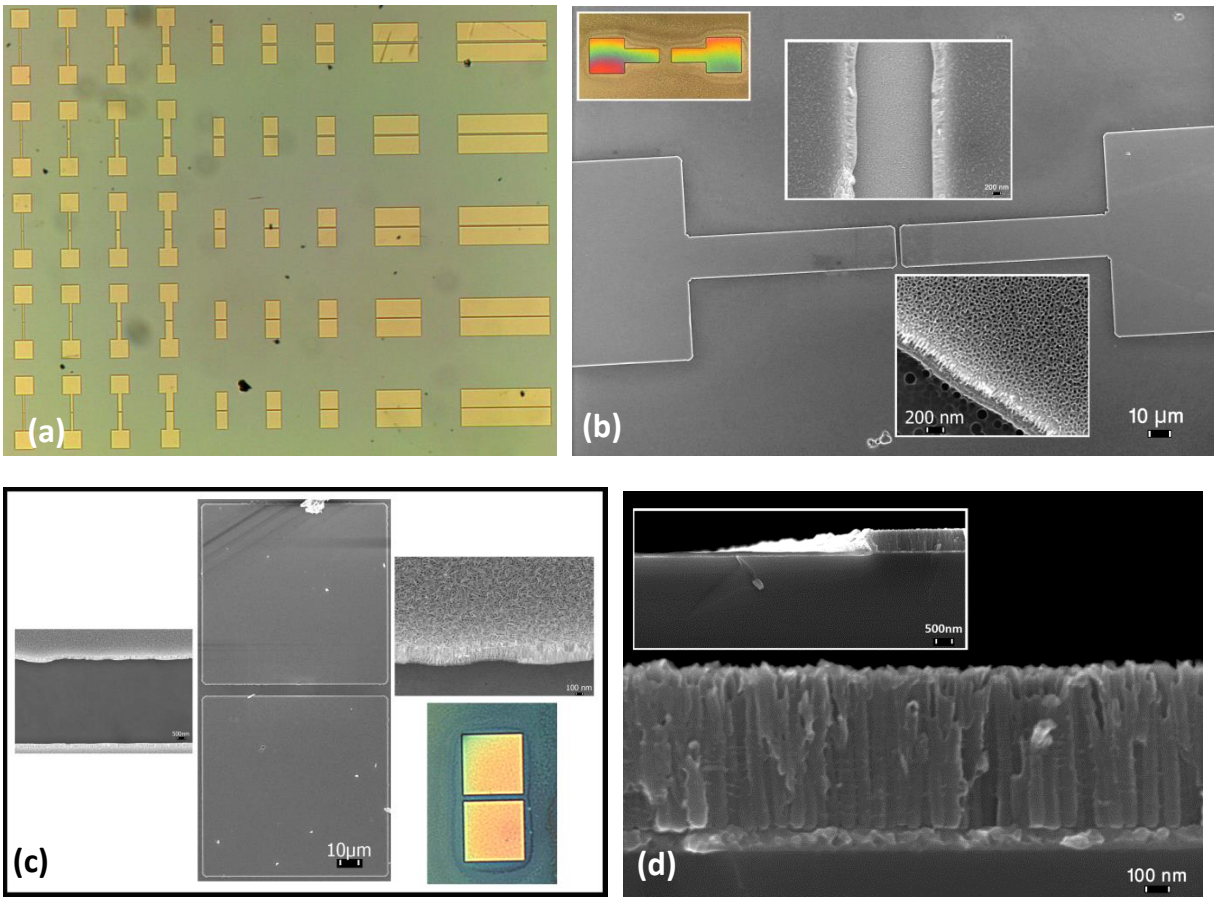

Fig. 4 (a) Optical micrograph (10X magnification) of patterned Ti film onto Si wafer. (b) and (c) top view SEM and optical microscopy images and (d) cross-sectional SEM images of TiO_2 nanotube arrays grown without any electrode connection to the sample.

Herein we also show that the applied magnetic field can be used to control the morphology of the TiO_2 nanotube arrays grown on the Ti sample connected to the anode and placed in front of the cathode electrode. The anodization rate (determinative of nanotube length) can be readily modulated by manipulating the magnetic field strength. Fig. 5a shows the current density between the cathode and anode (both Ti foils) with, and without applied magnetic field, during anodization for anode surface areas of 0.77 and 1.16 cm^2 respectively. It may be observed that the applied magnetic field during anodization decreases the Faradaic efficiency of nanotube formation at the anode due to the Lorentz force-induced deflection of ions towards LHS and RHS, hence reducing the number of the ions reaching the anode. This manifests itself in the lower anodization current density (Fig. 5a) during the pitting and nucleation stages of nanotube growth, and in the lower nanotube lengths achieved (Figs. 5b and 5c) when a magnetic field is present. This points to the ability of the magnetic field to control the length of nanotubes grown on the front Ti foil (electrical anode) without changing any other anodization parameter.

The 1 cm inter-electrode distance resulted in high electric fields in the electrolyte, which promoted the full dissociation of the dissolved salt. Since a 1-cm cuvette was used as the electrochemical cell, a small amount of the electrolyte was present during anodization (only about 3.8 mL). Due to the above two factors, the electrolyte became fully ionized several minutes into the anodization process if the anode surface area was large enough (1.16 cm^2 in this case) and the electrolyte turned highly conductive. The resulting high currents raised the electrolyte temperature to a level where the cuvette melted and nanotube arrays onto front foil were damaged due to being harshly attacked by fluoride ions. For the utilized setup configuration and the applied voltage of 50 V we found the optimum anode surface area to be in the range of 0.8 to 1.1 cm^2 beyond which despite generating TiO_2 nanotube arrays on the LHS foil (in the

presence of the magnetic field), nanotube arrays on the front Ti foil anode get damaged. If the anode surface area is smaller than 0.8 cm^2, the nanotube array onto LHS Ti sample is not generated because the current density is too small to be efficiently deflected towards the left sample by the Lorentz force ($\vec{F} = q\vec{v} \times \vec{B}$). For anode surface areas within the optimum range, TiO_2 nanotubes are grown onto both front foil (electrical anode) and Ti-coated LHS samples (no electrode connection) using magnetic-field-assisted anodization.

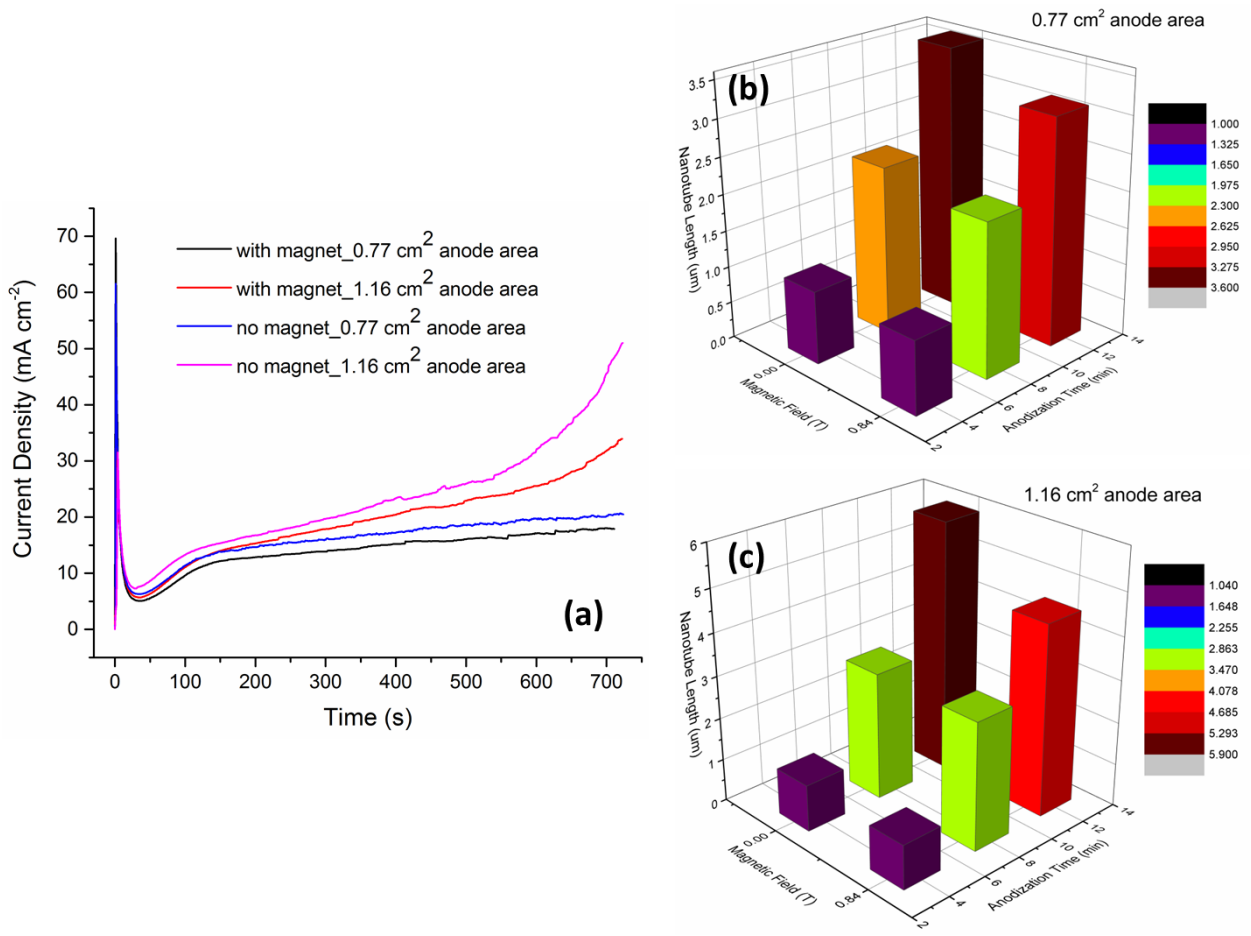

Fig. 5 (a) Current density plots during anodization of titania nanotube arrays for 0.77 and 1.16 cm^2 anode areas with/without applied magnetic field (b, c) Variation of nanotube length as a function of magnetic field strength and anodization duration for sample areas of 0.77 cm^2 and 1.16 cm^2 respectively.

Conclusions

We believe magnetic-field-assisted electrochemical anodization to be superior to the conventional anodization method since addresses many of its drawbacks. First of all, the sample (Ti foil or Ti coated substrate) is fully immersed into the electrolyte allowing utilization of its full area which is more cost effective. It also enables us to mount very small sized samples and grow titania nanotube arrays without any electrode connection on patterned substrates of any conductivity. Consequently, Ti film continuity is not needed during nanotube growth. This is of special importance for growing TiO_2 nanotubes onto small electronic chips or lab-on-a-chip devices. Traditionally, the Ti metal needed to be deposited everywhere on the substrate as a blanket film to provide the required conductivity for anodization process. Patterning the nanotubes after their growth, is a huge challenge when dealing with very small gaps and hitherto prevented the integration of TNT arrays with MEMS devices, porous substrates and substrates containing nanostructures such as oriented nanotube/nanowire/nanopore arrays of metals, dielectrics and semiconductors. Therefore demonstrated magnetic field-assisted electroless anodization process greatly expands the type of substrates on which TNT arrays may be formed. Since the sampl is not partially out of the electrolyte, no precaution is required to tackle the faster anodization issue at electrolyte/air interface. This will open a window towards much easier incorporation of TiO_2 nanotube arrays onto MEMS devices, chip-sized supercapacitors, microelectrocatalysts, etc. and also enable improved interfacing of nanotubes with the macroscale.

The magnetic field is an anodization parameter which can be used for morphology control of the fabricated TiO_2 nanotube arrays, and may also be easily extended to the formation

of other nanostructured valve metals such as Al_2O_3, HfO_2, ZrO_2, Ta_2O_5, etc. The Lorentz-force driven electroless anodization demonstrated by us may also provide deep insights into the anodization process. For instance, field-assisted migration was found to be unimportant to the electroless anodization process.

Acknowledgements

Authors thank NSERC, CFI, Alberta SEGP and NRC for funding/equipment support. AM acknowledges scholarship support from Alberta Innovates Technology Futures (AITF).

References

1. A. Mohammadpour and K. Shankar, *Journal of Materials Chemistry*, 2010, 20, 8474-8477.
2. S. Yoriya and C. A. Grimes, *Langmuir*, 2010, 26, 417-420.
3. S. P. Albu and P. Schmuki, *Phys. Status Solidi-Rapid Res. Lett.*, 2010, 4, 215-217.
4. A. Mohammadpour, P. R. Waghmare, S. K. Mitra and K. Shankar, *Acs Nano*, 2010, 4, 7421-7430.
5. B. Chen and K. Lu, *Langmuir*, 2012, 28, 2937-2943.
6. X. J. Zhang, F. Han, B. Shi, S. Farsinezhad, G. P. Dechaine and K. Shankar, *Angewandte Chemie-International Edition*, 2012, 51, 12732-12735.
7. C. T. Yip, H. T. Huang, L. M. Zhou, K. Y. Xie, Y. Wang, T. H. Feng, J. S. Li and W. Y. Tam, *Advanced Materials*, 2011, 23, 5624-+.
8. J. Lin, K. Liu and X. F. Chen, *Small*, 2011, 7, 1784-1789.
9. G. K. Mor, K. Shankar, M. Paulose, O. K. Varghese and C. A. Grimes, *Nano Letters*, 2006, 6, 215-218.
10. M. Paulose, K. Shankar, O. K. Varghese, G. K. Mor and C. A. Grimes, *Journal of Physics D-Applied Physics*, 2006, 39, 2498-2503.
11. D. Kuang, J. Brillet, P. Chen, M. Takata, S. Uchida, H. Miura, K. Sumioka, S. M. Zakeeruddin and M. Gratzel, *Acs Nano*, 2008, 2, 1113-1116.
12. J. R. Jennings, A. Ghicov, L. M. Peter, P. Schmuki and A. B. Walker, *Journal of the American Chemical Society*, 2008, 130, 13364-13372.
13. T. Stergiopoulos, A. Ghicov, V. Likodimos, D. S. Tsoukleris, J. Kunze, P. Schmuki and P. Falaras, *Nanotechnology*, 2008, 19, 7.
14. K. Shankar, G. K. Mor, M. Paulose, O. K. Varghese and C. A. Grimes, *Journal of Non-Crystalline Solids*, 2008, 354, 2767-2771.
15. O. K. Varghese, M. Paulose and C. A. Grimes, *Nature nanotechnology*, 2009, 4, 592-597.
16. A. Vomiero, V. Galstyan, A. Braga, I. Concina, M. Brisotto, E. Bontempi and G. Sberveglieri, *Energy & Environmental Science*, 2011, 4, 3408-3413.
17. G. K. Mor, O. K. Varghese, M. Paulose, K. Shankar and C. A. Grimes, *Solar Energy Materials and Solar Cells*, 2006, 90, 2011-2075.

18. K. Shankar, J. I. Basham, N. K. Allam, O. K. Varghese, G. K. Mor, X. J. Feng, M. Paulose, J. A. Seabold, K. S. Choi and C. A. Grimes, *Journal of Physical Chemistry C*, 2009, 113, 6327-6359.
19. K. Shankar, G. K. Mor, H. E. Prakasam, S. Yoriya, M. Paulose, O. K. Varghese and C. A. Grimes, *Nanotechnology*, 2007, 18, 11.
20. B. Chen, J. B. Hou and K. Lu, *Langmuir*, 2013, 29, 5911-5919.
21. X. H. Lu, G. M. Wang, T. Zhai, M. H. Yu, J. Y. Gan, Y. X. Tong and Y. Li, *Nano Lett.*, 2012, 12, 1690-1696.
22. H. Wu, D. D. Li, X. F. Zhu, C. Y. Yang, D. F. Liu, X. Y. Chen, Y. Song and L. F. Lu, *Electrochim. Acta*, 2014, 116, 129-136.
23. H. Zhou and Y. R. Zhang, *J. Phys. Chem. C*, 2014, 118, 5626-5636.
24. G. K. Mor, M. A. Carvalho, O. K. Varghese, M. V. Pishko and C. A. Grimes, *J. Mater. Res.*, 2004, 19, 628-634.
25. M. Paulose, O. K. Varghese, G. K. Mor, C. A. Grimes and K. G. Ong, *Nanotechnology*, 2006, 17, 398-402.
26. B. M. Rao and S. C. Roy, *The Journal of Physical Chemistry C*, 2013, 118, 1198-1205.
27. J. Park, S. Bauer, A. Pittrof, M. S. Killian, P. Schmuki and K. von der Mark, *Small*, 2012, 8, 98-107.
28. J. Park, S. Bauer, K. von der Mark and P. Schmuki, *Nano Lett.*, 2007, 7, 1686-1691.
29. S. Oh, K. S. Brammer, Y. S. J. Li, D. Teng, A. J. Engler, S. Chien and S. Jin, *Proceedings of the National Academy of Sciences*, 2009, 106, 2130-2135.
30. S. J. Bao, C. M. Li, J. F. Zang, X. Q. Cui, Y. Qiao and J. Guo, *Advanced Functional Materials*, 2008, 18, 591-599.
31. C. X. Wang, L. W. Yin, L. Y. Zhang and R. Gao, *J. Phys. Chem. C*, 2010, 114, 4408-4413.
32. K.-S. Mun, S. D. Alvarez, W.-Y. Choi and M. J. Sailor, *ACS Nano*, 2010, 4, 2070-2076.
33. P. Kar, A. Pandey, J. J. Greer and K. Shankar, *Lab Chip*, 2012, 12, 821-828.
34. K. C. Popat, M. Eltgroth, T. J. LaTempa, C. A. Grimes and T. A. Desai, *Small*, 2007, 3, 1878-1881.
35. K. Gulati, M. S. Aw and D. Losic, *Nanoscale Res. Lett.*, 2011, 6, 6.
36. Y. Y. Song, F. Schmidt-Stein, S. Bauer and P. Schmuki, *Journal of the American Chemical Society*, 2009, 131, 4230-+.
37. P. Granitzer, K. Rumpf, T. Ohta, N. Koshida, P. Poelt and M. Reissner, *Nanoscale Research Letters*, 2012, 7, 4.
38. T. Nakagawa, H. Koyama and N. Koshida, *Applied Physics Letters*, 1996, 69, 3206-3208.
39. B. Gelloz, M. Masunaga, T. Shirasawa, R. Mentek, T. Ohta and N. Koshida, *ECS Transactions*, 2008, 16, 195-200.
40. Y. Morishita, S. Kawai, J. Sunagawa and T. Suzuki, *Electrochemical and Solid State Letters*, 2001, 4, G4-G6.